



ELSEVIER

Computer Physics Communications 112 (1998) 67–79

Computer Physics
Communications

Computation of photoelectron and Auger-electron diffraction I. Preparation of input data for the cluster calculation PAD1

X. Chen, D.K. Saldin¹

Department of Physics and Laboratory for Surface Studies, University of Wisconsin-Milwaukee, P.O. Box 413, Milwaukee, WI 53201, USA

Received 10 December 1996; revised 1 December 1997

Abstract

We describe the theory and implementation of multiple scattering cluster calculations of angle-resolved core-level photoelectron and Auger-electron diffraction intensities based on a concentric-shell algorithm (CSA). In this paper, we describe the first of a series of three computer programs which implement the calculations. In the present program, sorting algorithms are used to arrange atoms by their symmetry groups and into a series of concentric shells, as required by the CSA. For maximum user-friendliness, all input parameters may be specified in a self-explanatory file, which contains information about the cluster and the experimental parameters. © 1998 Elsevier Science B.V.

PACS: 61.14.Qp; 61.14.Dc; 68.35.Bs

Keywords: Angle resolved; Core-level; Photoelectron; Auger; Electron diffraction; Surface structure; Multiple scattering; Electron spectroscopy

PROGRAM SUMMARY

Title of program: PAD1

Catalogue identifier: ADHZ

Program Summary URL:

<http://www.cpc.cs.qub.ac.uk/cpc/summaries/ADHZ>

Program obtainable from: CPC Program Library, Queen's University of Belfast, N. Ireland

Licensing provisions: none

Computer for which the program is designed and others on which it is operable: DEC-alpha and Silicon Graphics workstations, and CRAY and NEC supercomputers

Operating systems under which the program has been tested: UNIX

Program language used: FORTRAN-77

Memory required to execute with typical data: 1.9 mega-words

No. of bits in a word: 64

No. of processors used: 1

Has the code been vectorised or parallelized? No

No. of bytes in distributed program, including test data, etc.: 23965

¹ Corresponding author; e-mail: dksaldin@csd.uwm.edu.

Distribution format: uuencoded compressed tar file

Keywords: Angle resolved, core-level, photoelectron, Auger, electron diffraction, surface structure, multiple scattering, electron spectroscopy

Nature of physical problem

PAD1 generates a concentric shell cluster and switch parameters which will be used as include and control files for the second and third programs, PAD2 and PAD3, respectively, of this suite. The latter programs perform multiple scattering cluster calculations of angle-resolved core-level photoelectron and Auger-electron diffraction intensities via a concentric-shell algorithm (CSA).

Method of solution

Use of sorting algorithms to classify a cluster of atoms into se-

ries of concentric-shell clusters. Within each shell atoms are arranged in symmetrically equivalent groups, a format required by the second program PAD2 of this suite. This classification of atoms enables significant savings of both memory and computer time requirements.

Restrictions

For photoelectron diffraction, emission from only *s*, *p*, *d*, and *f* core states are allowed by the present code.

Typical running time

0.196 seconds on a Silicon Graphics Indigo² computer with an R10000 processor for the test data set.

Unusual features of the program

For correct results, this program should be compiled using the DOUBLE PRECISION option of the compiler.

LONG WRITE-UP

1. Introduction

In recent years, diffraction patterns arising from the emission of atomic core electrons have played an increasing role in surface structure determination. Examples of such techniques are core-level photoelectron diffraction (PD) and Auger-electron diffraction (AD). In part this is due to the greater availability of synchrotron radiation sources. The chemical specificity of the energies of the emitted electrons makes such techniques particularly useful for the study of multi-component surfaces and interfaces.

There exist several computer codes for calculating photoelectron diffraction based on multiple-scattering theory, but few have been made accessible to the public in a user-friendly form. The concentric shell algorithm (CSA), developed originally for low energy electron diffraction (LEED) [1,2], was subsequently applied to Auger and photoelectron diffraction [3]. This technique has proved its worth through many published applications [4–11] in which results of the calculations have been compared with measured diffraction patterns.

The CSA performs a full multiple-scattering calculation amongst all the atoms in a cluster around an electron emitter. Unlike techniques based on a decomposition of the surface into a set of two-dimensional periodic layers [12–15], it makes no assumption of long-range order amongst different emitters. The layer-based techniques perform an entire multiple-scattering calculation for each separate direction of detection, and their computational time scales linearly with the number of detected data points. In contrast, a unique feature of the CSA scheme is that the final wave-field is expressed as a sum of spherical waves centered on a single origin, namely the position of the electron emitter. Thus the entire angular distribution of detectable electrons is calculated simultaneously.

The CSA algorithm classifies the cluster of scattering atoms into a set of concentric shells centered at the emitter. In order to speed up the calculations, the shells need to be specified according to a well-defined prescription that allows an optimum division of labour between the evaluation of intra- and inter-shell multiple scattering. In addition, the coordinates of atoms within a particular shell are specified in such a way as to facilitate the use of symmetry to further speed up the calculations.

In this paper (paper I) we describe the first (PAD1) of a suite of three computer programs that calculates angle-resolved PD and AD intensities, as measured under a variety of different common experimental configurations. The function of the present program is to read the basic input data, as specified in a user-friendly form, to generate the parameters needed to perform the calculations in papers II [25] and III [26] of this sequence.

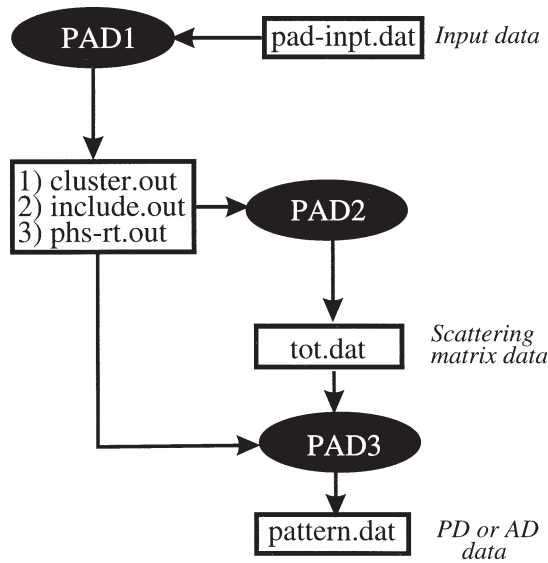


Fig. 1. Flow chart describing the sequence and data exchanges amongst the PAD programs.

These parameters include the specification of the dimensions of arrays needed for the next two programs (PAD2 and PAD3) of our suite.

One of the important functions of the PAD1 program is the generation of the coordinates and arrangement of atoms into concentric-shells as required for the cluster calculation performed by the PAD2 program. It should be noted that the concentric-shell cluster generated by the PAD1 program may be used also by programs that employ similar cluster algorithms for the calculation of LEED intensities [1,2], and X-ray absorption near-edge structures (XANES) [16,17].

A further function of PAD1 is to take input zero-temperature atomic phase shifts, and from them to generate finite temperature phase shifts for the temperature specified in the input file.

The PAD1 program also evaluates the amplitudes of the spherical-wave components (in a frame of reference tied to the direction of the magnetic vector potential of the exciting radiation) of the wavefunction of a photoelectron immediately after its emission from an atom, using the data on the magnitudes of the radial matrix elements supplied as input. These spherical-wave amplitudes are written onto an output file for use by the PAD3 program.

2. Overview of PAD programs

To simulate angle-revolved electron diffraction with the PAD programs, it is necessary to run the programs PAD1, PAD2, and PAD3 in the sequence specified in the flow chart of Fig. 1. The sequence is important, since the correct compilation of PAD2 and PAD3 is possible only after PAD1 is executed. This is due to the fact that an include file generated by PAD1 determines the sizes of the arrays used by PAD2 and PAD3 during their execution, for the specified problem. To summarize, PAD1 calculates the concentric-shell cluster and control parameters required for PAD2, and the amplitudes of the outgoing spherical waves radiated from the photoemitter, as required by PAD3. PAD2 calculates the cluster scattering matrix that describes the effects of the electron's multiple scattering by the atoms near the photoemitter, and finally, PAD3 evaluates and writes out the PD intensities for comparison with the results of experiments performed under a variety of conditions.

3. Theory of atomic photoemission

An atomic core electron in a state $|\psi_{n,L_c}\rangle$ of principal quantum number n , and angular momentum quantum numbers $L_c \equiv (l_c, m_c)$, is capable of being excited into an unbound state $|\psi(E)\rangle$ of positive energy E by the absorption of a photon of energy greater than its binding energy. On a muffin-tin model of a flat interstitial potential, $V = 0$, and spherically averaged atomic potentials of finite radius, the wavefunction of the excited electron of energy E may be written

$$\psi(E, \mathbf{r}') = \int d\mathbf{r}'' G^+(\mathbf{r}', \mathbf{r}'', E) \widehat{\Delta}(\mathbf{r}'') \psi_{n,L_c}(\mathbf{r}''), \quad (1)$$

where \mathbf{r}' and \mathbf{r}'' are position vectors,

$$\widehat{\Delta}(\mathbf{r}'') = \frac{-i}{\omega} \mathbf{A} \cdot \nabla V(\mathbf{r}'') \quad (2)$$

is the “potential form” of the electromagnetic perturbation operator, in Hartree atomic units, \mathbf{A} the magnetic vector potential of the exciting radiation, ω its angular frequency, ∇ the vector gradient operator, and V the atomic potential. Some prior work on the photoemission matrix elements [18] has used instead the “position form” of this operator,

$$\widehat{\Delta}(\mathbf{r}'') = i\omega \mathbf{A} \cdot \mathbf{r}'' . \quad (3)$$

It can be shown that the two forms (2) and (3) are equivalent.

The retarded Green’s function

$$G^+(\mathbf{r}', \mathbf{r}'', E) = -ik \sum_L R_l(kr_<) R_l^{(+)}(kr_>) Y_L(\hat{\mathbf{r}}') Y_L^*(\hat{\mathbf{r}}'') , \quad (4)$$

where $k(= \sqrt{2E})$ is the wavenumber of the emitted electron in the interstitial region, $L \equiv (lm)$ are angular momentum quantum numbers, Y_L a spherical harmonic, $R_l(kr)$ is the regular solution of the radial Schrödinger equation for the atom, which matches on to the function

$$j_l(kr) \cos \delta_l - n_l(kr) \sin \delta_l , \quad (5)$$

and $R_l^{(+)}(kr)$ is the irregular solution which matches on to

$$h_l^{(1)}(kr) e^{i\delta_l} \quad (6)$$

at the muffin-tin boundary. In the above expressions, j_l , n_l , and $h_l^{(1)}$ are the spherical Bessel, Neumann, and Hankel function of the first kind of order l , and δ_l is an atomic phase shift of angular momentum l .

Substituting (4) into (1) and using (2), we see that, beyond the muffin-tin radius, the emitted electron wavefunction may be written in the form

$$\psi(E, \mathbf{r}') = \sum_L B_{nL_c,L}^{(0)'} h_l^{(1)}(kr') Y_L(\hat{\mathbf{r}}') \quad (7)$$

in a frame of reference $\mathbf{a}' = (x', y', z')$, with the z' axis taken in the direction of the magnetic vector potential \mathbf{A} . We may term this the laboratory reference frame. For core-level photoemission from the state $|\psi_{n,L_c}\rangle$, this amplitude may be evaluated in terms of the polar coordinates (r', θ', ϕ') of this reference frame as

$$B_{nL_c,L}^{(0)'} = -\frac{Ak}{\omega} \langle L | \cos \theta' | L_c \rangle Q_{l,m_c} e^{i\delta_l} , \quad (8)$$

with

$$Q_{l,nl_c} = \int R_l(r) \frac{\partial V}{\partial r} \phi_{nl_c}(r) dr, \quad (9)$$

and the core wavefunction written as

$$\langle \mathbf{r} | \psi_{n,L_c} \rangle = \phi_{nl_c}(r) Y_{L_c}(\mathbf{r}). \quad (10)$$

Thus the emitted electron wavefunction may be written as a sum (7) of outgoing spherical waves of amplitudes $B_{nL_c,L}^{(0)'}$ which involve a product of a radial matrix element Q_{l,nl_c} and the angular integral

$$\langle L | \cos \theta' | L_c \rangle \equiv \int Y_L^*(\Omega') \cos \theta' Y_{L_c}(\Omega') d\Omega', \quad (11)$$

where Ω' represents the pair of polar and azimuthal angles (θ', ϕ') . This integral may be evaluated with the aid of the relationship [19]

$$\cos \theta' Y_{lm}(\Omega') = a_{l,m} Y_{l+1,m}(\Omega') + a_{l-1,m} Y_{l-1,m}(\Omega'), \quad (12)$$

where

$$a_{lm} = \sqrt{\frac{(l+1)^2 - m^2}{(2l+1)(2l+3)}}. \quad (13)$$

Substituting (13) and (12) into (11), and making use of the orthonormality of spherical harmonics, it may be seen that

$$\langle L | \cos \theta' | L_c \rangle = (a_{l_c,m_c} \delta_{l,l_c+1} + a_{l_c-1,m_c} \delta_{l,l_c-1}) \delta_{m,m_c}, \quad (14)$$

which gives rise to the selection rules $l = l_c \pm 1$ and $m = m_c$ for the atomic transition.

Thus the essential elements in the calculation of the spherical-wave amplitudes $B_{nL_c,L}^{(0)'}$ of the photoemitted electron are the angular matrix element $\langle L | \cos \theta' | L_c \rangle$, which is evaluated from (14), and the radial matrix element Q_{l,nl_c} , which may be read in from the output of another computer program (see Section 5, below).

In an atomic photoemission process, the magnetic vector potential \mathbf{A} of the incident electromagnetic radiation provides a convenient polar axis for the spherical harmonic expansion of the emitted electron wavefunction. For the evaluation of the subsequent scattering of this wave by a surrounding cluster of atoms, however, it is more convenient to re-express the spherical wave amplitudes $B_{nL_c,L}^{(0)'}$ in terms of those $B_{nL_c,L}^{(0)}$ referred to a polar axis fixed relative to the atomic cluster. This conversion is performed by the PAD3 program and is described in paper III of this series.

4. Theory of atomic Auger emission

An atomic Auger process may be thought of occurring in three steps: an initial core-level ionization, followed by a transition of an electron from a higher energy state into that core hole, which in turn is accompanied by the transfer of the energy loss of that electron to a third (and weakly-bound) electron, which is emitted from the atom. Even if the second and/or third electrons were initially in valence-band states in a solid, the localization of the initial core hole would tend to make all three processes localized near the atom. Consequently, even in such a case, an Auger process may be thought of as essentially atomic, and consequently characterized by atomic Auger matrix elements.

The calculation of Auger matrix elements is considerably more complicated than that of the corresponding photoemission quantities described in the last section. Computations for particular transitions have been reported, for example, by Asaad [20,21] and Hörmandinger et al. [22] and the topic of Auger spectroscopy for surface studies has been reviewed by Weissmann and Müller [23]. The initial core hole of an Auger process may be created by a variety of means, e.g. absorption of a photon, or inelastic scattering of an incident electron. The directional nature of the initial excitation process can cause an anisotropy in the emission of the final Auger electron, but unlike the case of atomic photoemission, this anisotropy is usually too small to be observed from a solid-state source after the problematic background subtraction [23]. Consequently, the wavefield of an Auger electron emitted into the angular momentum channel L may be written

$$B_{\text{Aug},L}^{(0)} h_l^{(1)}(kr) Y_L(\hat{\mathbf{r}}), \quad (15)$$

where, unlike the case of atomic photoemission, the polar axis used to define the spherical harmonic Y_L may be taken directly to be one fixed relative to the crystal. The amplitudes $B_{\text{Aug},L}^{(0)}$ may be deduced from calculations of Auger transition probabilities, e.g. [20,21], or even from fits to experimental data [4]. Isotropic emission may be modelled by assuming that

$$B_{\text{Aug},L}^{(0)} \equiv B_{\text{Aug},l}^{(0)}, \quad (16)$$

i.e. that the amplitudes of the emitted Auger electrons of the same angular momentum channel l , but different magnetic quantum numbers m are the same, and by summing the contributions from those different m incoherently (see Section 3 of paper III).

5. Program structure of PAD1

The program PAD1 performs its calculations in 4 stages, as described below.

Stage 1 reads input control parameters from unit 4, `pad-inpt.dat`, which is a self-explanatory file that contains information about the crystallographic structure, zero-temperature atomic phase shifts δ_l , radial matrix elements $Q_{l,nl}$, and the experimental configuration and type of calculation to be attempted. A good source of these radial photoemission matrix elements is the MUFPO program developed by Pendry and co-workers [24]. An alternative source is the paper by Goldberg et al. [18], which contains tabulated values of these matrix elements for some selected elements, as calculated using the “position form” (3) of the perturbation operator $\hat{\Delta}(\mathbf{r})$. The form used is specified in the input file `pad-inpt.dat` by the value of the parameter `IMTX`.

Stage 2 calculates phase shifts from the zero-temperature phase shifts read from FORTRAN unit 4 in Stage 1, as a function of temperature. This is done by the method suggested by Pendry [24], with some modifications for converting the phase shifts at 0 K into the phase shifts at room temperature, including the effects of surface atom vibrations.

Stage 3 sorts a cluster of atoms centered at an emitter by their chemical species and distances from the emitter, and classifies the atoms into series of concentric shells centered on the emitter. Atoms within each shell are further subdivided into sets related by rotational and mirror symmetry operations. The maximum angular momentum quantum numbers for the single-center expansions of the wavefunctions in terms of spherical harmonics are also determined at this stage.

Stage 4 outputs several files, used as include and control files for the PAD2 and PAD3 programs to carry out multiple scattering calculations. A concentric-shell cluster of atoms, amplitudes, $B_L^{(0)l}$, of the spherical waves emitted by the atomic photoemission process, and a specification of the experimental geometry and the polarization of the incident X-rays are also written out on FORTRAN unit 5. At this stage, the dimensions of the arrays used in the calculation of the cluster scattering matrix and control parameters are output from FORTRAN unit 6. The finite temperature phase shifts are output on unit 8.

Table 1
Input parameters

| | |
|----------------------------|--|
| (a) JOBTITLE | Title of the job as a heading. |
| (b) MID | Number of atom species in a surface unit cell. |
| (c) NATOM(I) | Number of atoms of each species I (=1,MID) in the 2D unit cell. |
| (d) A_x, A_y, B_x, B_y | Translational vectors A and B of the 2D unit cell (\AA). |
| (e) NREL | Switch for fractional (NREL=0) or absolute (NREL=1) coordinates for CLL_X, and CLL_Y only. |
| (f) CLL_X(I,J), CLL_Y(I,J) | Coordinates of all the atoms (I,J) in the unit cell CLL_Z(I,J). N.B. Put emitter first! (absolute coordinates in \AA). |
| (g) IAXISP | Degree of rotational symmetry about z-axis through emitter. |
| (h) MIRP | x-y mirror plane through emitter? No (MIRP=0) or Yes (MIRP=1). |
| (i) NGENO | Experiment type: AD0 (NGEO=0), PD1 (NGEO=1), PD2 (NGEO=2), PD3 (NGEO=3), PD4 (NGEO=4). |
| (j) THETA, PHI | X-ray ϵ vector direction ($\theta_\epsilon, \phi_\epsilon$) in sample reference frame. Note: Used by PD1 or PD3 mode only! |
| (k) VIN | Muffin-tin zero energy relative to the vacuum (eV). |
| (l) ENERGY | Kinetic energy (<i>in vacuo</i>) of the emitted electron (eV). |
| (m) EMFP | Electron mean-free-path (\AA). If EMFP=0 use universal curve. |
| (n) ECOPE | Binding energy of electron core state. |
| (o) NSTATE | Number of l channels of the emitted electron. |
| (p) IMTX | Source of matrix elements. For PD: MUFPTOT (IMTX=0), Ref. [18] (IMTX=1); for AD (IMTX>1). |
| (q) LF(I), WGHT(I) | Emission angular momenta and matrix elements: (l, Q_{l,nl_c}), ($l = l_c - 1, l_c + 1$) for PD; or ($L, B_{Aug,L}^{(0)}$), ($l=0, NSTATE-1$) for AD. |
| (r) IFWD | Switch between full multiple scattering (MS): IFWD=0; outward scattering approximation (OS) IFWD=1; and single scattering (SS) IFWD=2. |
| (s) RMAX | Radius of the atom cluster (\AA). |
| (t) ITHA0, ITHA1, ITSTP | Initial and final polar angles of detection and step between successive values (degrees). |
| (u) IPHI0, IPHI1, IPSTP | Same as above except for azimuthal angles. |
| (v) SRFPNT | Surface barrier height above emitter (\AA). |
| (w) DTEP(I) | Debye temperatures for species I (=1,MID) (K). |
| (x) ATMASS(I) | Atomic mass for species I (=1,MID) (moles). |
| (y) LMAX | Maximum angular momentum quantum number of scattering phase shifts. |
| (z) PHS(I,J) | Phase shifts at 0K (radians), for species I (=1,MID) with angular momentum J (=0,LMAX). |

6. Input parameters

Input parameters, as listed in Table 1, are contained in a file, `pad-inpt.dat`. This specified data includes the crystallographic parameters, such as the 2D surface unit cell, the atomic species, the symmetry and size of the cluster of atoms around the emitter, the atomic phase shifts, the radial photoemission matrix elements, the binding energy of the core electron, the sample's inner potential relative to the vacuum, the type of experiment, the kinetic energy of the emitted electron, the scattering model, and the polar and azimuthal angles of the detector in the sample's reference frame.

In the current package, four types of PD experiments are incorporated in the code. The type of experiment simulated by the program is determined by the value of the input parameter NGENO. Paper III of this series describes the details of these four types of the experimental geometries.

IFWD is also a switch parameter, which allows PAD2 to perform a cluster calculation based on a full multiple scattering (MS) theory (IFWD=0), an outward multiple scattering (OS) approximation (IFWD=1), or a single scattering (SS) approximation (IFWD=2). For electron kinetic energies above about 100 eV, the forward-peaked nature of atomic scattering factors may be exploited by the use of OS approximation, which generally simulates the diffraction patterns quite well at such energies. Such an approximation may speed up the computation, and requires less computer memory by about an order of a magnitude. With typical computer

resources available at present, this is necessary for larger cluster calculations at higher electron kinetic energies.

7. Output

The output from the PAD1 program is written on unit 5 (`cluster.out`), unit 6 (`include.out`), and unit 8 (`phs-rt.dat`). Each of these files has a unique function and carries information to the PAD2 and PAD3 programs to perform Auger- or photoelectron diffraction simulations for a selected experimental geometry.

`cluster.out` contains information about the concentric-shell cluster which may be read by both PAD2 and PAD3. For photoemission, it also contains the amplitudes $B_{L,L_c}^{(0)}$ of the initially emitted electrons, and the corresponding quantities, $B_{\text{Aug},L}^{(0)}$, for Auger emission, as needed by the PAD3 program. Note that both of these sets of quantities are written out by this program regardless of whether the input quantity IMTX specifies Auger or photoemission. The PAD3 program uses only the appropriate set of amplitudes for the calculation being performed.

`include.out` defines sizes of the arrays for both PAD2 and PAD3. This is used as an INCLUDE file by the PAD2 and PAD3 programs during compilation. This file also passes over the values of the switches originally specified in the `pad-inpt.dat` file. These switches determine the types of calculation performed by the PAD2 and PAD3 programs.

`phs-rt.dat` is a data file containing atomic scattering phase shifts at room temperature.

8. Test run

The test run calculates core-level O-1s PD, for an electron kinetic energy of 60 eV, for experiment type of PD3, illustrated in Fig. 1c of paper III of this set of papers. The O atom is assumed to occupy the 4-fold hollow site on a Ni(001) surface. In this run the full multiple-scattering option (IFWD=0) is assumed.

Acknowledgements

D.K.S. wishes to acknowledge support for this work from the U.S. National Science Foundation (Grant No. DMR-9320275) and from the Donors of the Petroleum Research Fund, administered by the American Chemical Society. X.C. is grateful to Drs. S. Kono and T. Abukawa of Research Institute for Scientific Measurements of Tohoku University, Japan, for stimulating discussions and for suggestions for writing and modifying this suite of programs.

References

- [1] J.B. Pendry, in: Determination of Surface Structures by LEED, P.M. Marcus, F. Jona, eds. (Plenum, New York, 1984) p. 3.
- [2] D.K. Saldin, J.B. Pendry, Surf. Sci. 162 (1985) 941. (1985).
- [3] D.K. Saldin, G.R. Harp, X. Chen, Phys. Rev. B 48 (1993) 8234.
- [4] D.K. Saldin, G.R. Harp, B.P. Tonner, Phys. Rev. B 45 (1992) 9629.
- [5] X. Chen, G.R. Harp, D.K. Saldin, J. Vac. Sci. Technol. A 12 (1994) 428.
- [6] S. Varma, X. Chen, I. Davoli, J. Zhang, D.K. Saldin, B.P. Tonner, Surf. Sci. 314 (1994) 145.
- [7] X. Chen, H.W. Yeom, T. Abukawa, Y. Takakuwa, T. Shimatani, Y. Mori, A. Kakizaki, S. Kono, J. Electr. Spectrosc. Relat. Phenom. 80 (1996) 147.
- [8] X. Chen, T. Abukawa, J. Tani, S. Kono, Phys. Rev. B 52 (1995) 12380.
- [9] X. Chen, T. Abukawa, J. Tani, S. Kono, Surf. Rev. Lett. 2 (1995) 795.
- [10] X. Chen, T. Abukawa, J. Tani, S. Kono, Surf. Sci. 357/358 (1996) 560.

- [11] X. Chen, D.K. Saldin, E.L. Bullock, L. Patthey, L.S.O. Johansson, J. Tani, T. Abukawa, S. Kono, *Phys. Rev. B* 55 (1997) R7319.
- [12] J.B. Pendry, *Surf. Sci.* 57 (1976) 679.
- [13] C.H. Li, S.Y. Tong, *Phys. Rev. Lett.* 40 (1978) 46.
- [14] C.H. Li, A.R. Lubinsky, S.Y. Tong, *Phys. Rev. B* 17 (1978) 3128.
- [15] S.Y. Tong, C.H. Li, in: *Chemistry and Physics of Solid Surfaces*, R. Vanselow, W. England, eds. (CRC, Boca Raton, 1982).
- [16] P.J. Durham, J.B. Pendry, C.H. Hodges, *Comput. Phys. Commun.* 29 (1982) 193.
- [17] D.D. Vvedensky, D.K. Saldin, J.B. Pendry, *Comput. Phys. Commun.* 40 (1986) 421.
- [18] S.M. Goldberg, S. Kono, C.S. Fadley, *J. Electr. Spectrosc. Relat. Phenom.* 21 (1981) 285.
- [19] See e.g. E.U. Condon, G.H. Shortley, in: *The Theory of Atomic Spectra* (Cambridge Univ. Press, Cambridge, 1935).
- [20] W.N. Asaad, *Nucl. Phys.* 44 (1963) 399.
- [21] W.N. Asaad, *Nucl. Phys.* 44 (1963) 415.
- [22] G. Hörmandinger, P. Weinberger, P. Marksteiner, J. Redinger, *Phys. Rev. B* 38 (1988) 1040.
- [23] R. Weissmann, K. Müller, *Surf. Sci. Rep.* 105 (1981) 251.
- [24] J.B. Pendry, *Low Energy Electron Diffraction* (Academic Press, London, 1974) p. 368.
- [25] G.R. Harp, Y. Ueda, X. Chen, D.K. Saldin, *Comput. Phys. Commun.* 112 (1998) 80, paper II.
- [26] X. Chen, G.R. Harp, Y. Ueda, D.K. Saldin, *Comput. Phys. Commun.* 112 (1998) 91, paper III.

TEST RUN INPUT

pad-inpt.dat: Input file for pad1.f

```

=====
      pad-inpt.dat: Input file for pad1.f (stream 4)
=====
(a)  NAME OF THE STRUCTURE:
Ni(001)P2X2-0
(b)  NUMBER OF ATOM SPECIES IN SURFACE UNIT CELL:
2
(c)  NUMBER OF ATOMS FOR EACH SPECIES IN THE CELL (EMITTER SPECIES FIRST):
1 , 16
(d)  TRANSLATION VECTORS FOR THE CELL (ANGSTROMS):
4.978 , 0.000
0.000 , 4.978
(e)  FRACTIONAL <0> OR ABSOLUTE <1> COORDINATES FOR X-Y:
0
(f)  ATOMIC COORDINATES (X,Y,Z) IN THE CELL (ABS CO-ORDS IN ANGSTROMS):
0.250 , 0.250 , 0.820          <- Emitter comes first!
0.000 , 0.000 , 0.000
0.500 , 0.000 , 0.000
0.000 , 0.500 , 0.000
0.500 , 0.500 , 0.000
0.250 , 0.250 , -1.760
0.250 , 0.750 , -1.760
0.750 , 0.250 , -1.760
0.750 , 0.750 , -1.760
0.000 , 0.000 , -3.520
0.500 , 0.000 , -3.520
0.000 , 0.500 , -3.520
0.500 , 0.500 , -3.520
0.250 , 0.250 , -5.280
0.250 , 0.750 , -5.280
0.750 , 0.250 , -5.280
0.750 , 0.750 , -5.280
(g)  ROTATIONAL SYMMETRY ABOUT Z-AXIS THROUGH EMITTER:
4
(h)  HORIZONTAL MIRROR PLANE THROUGH EMITTER? NO <0> YES <1>:
0
(i)  EXPERIMENT TYPE: AD <0>, PD1 <1>, PD2 <2>, PD3 <3>, PD4 <4>
3
(j)  X-RAY E-VECTOR DIRECTION, THETA AND PHI (DEGREES): USED BY PD1 & PD3
45.0 , 0.0
(k)  INNER POTENTIAL (eV):
-10.0
(l)  ELECTRON KINETIC ENERGY IN VACUO (eV):
50.0
(m)  ELECTRON MEAN-FREE-PATH (ANGSTROMS): IF ZERO, USE UNIVERSAL CURVE
0
(n)  BINDING ENERGY OF THE CORE-LEVEL STATE (eV):
-536.
(o)  NUMBER OF L CHANNELS OF ELECTRON FINAL STATE:
1
(p)  RADIAL MATRIX ELEMENTS FOR PE: MUFFPOT (0) REF[13] (1); AUGER (2)
0
(q)  (L , RADIAL MATRIX ELEMENT) PAIRS FOR EACH L CHANNEL:

```

```
1 , 1.0
(r) TYPE OF SCATTERING: MS <0> OS <1> SS <2>
0
(s) MAXIMUM RADIUS OF CLUSTER (ANGSTROMS):
7.
(t) INITIAL AND FINAL POLAR ANGLES AND A STEP (DEGREES):
0 , 90 , 1
(u) INITIAL AND FINAL AZIMUTHAL ANGLES AND A STEP (DEGREES):
0 , 360, 1
(v) SURFACE BARRIER DISTANCE ABOVE EMITTER (ANGSTROMS):
1.058
(w) DEBYE TEMPERATURE (KELVIN) (EMITTER SPECIES FIRST):
999. , 450.
(x) ATOMIC MASS (MOLES) (EMITTER SPECIES FIRST):
16.0 , 58.7
(y) MAXIMUM ANGULAR MOMENTUM OF ATOMIC PHASE SHIFTS (LMAX):
4
(z) Oxygen at 60 eV
3.83620, 1.92370, 0.33544, 0.032426, 0.00266
(z) Ni at 60 eV
8.10180, 5.89240, 3.00480, 0.293530, 0.04804

===== END OF pad-inpt.dat (VERSION 3) X. CHEN AND D. K. SALDIN, 08/96 =====
```

TEST RUN OUTPUT

phs-rt.out: Output file from pad1.f (stream 8)

Input file to pad2.f (stream 5)

```

(z)   Oxygen at 60 eV
0
20
0.20971E+01 0.70835E+00-0.12219E+01 0.32781E+00 0.36693E-01 0.31919E-02
0.20971E+01 0.37666E-01 0.41418E-01 0.18925E-01 0.17055E-02 0.34673E-04
0.21082E+01 0.70835E+00-0.12219E+01 0.32781E+00 0.36693E-01 0.31919E-02
0.21082E+01 0.37666E-01 0.41418E-01 0.18925E-01 0.17055E-02 0.34673E-04
0.21192E+01 0.70835E+00-0.12219E+01 0.32781E+00 0.36693E-01 0.31919E-02
0.21192E+01 0.37666E-01 0.41418E-01 0.18925E-01 0.17055E-02 0.34673E-04
0.21302E+01 0.70835E+00-0.12219E+01 0.32781E+00 0.36693E-01 0.31919E-02
0.21302E+01 0.37666E-01 0.41418E-01 0.18925E-01 0.17055E-02 0.34673E-04
0.21413E+01 0.70835E+00-0.12219E+01 0.32781E+00 0.36693E-01 0.31919E-02
0.21413E+01 0.37666E-01 0.41418E-01 0.18925E-01 0.17055E-02 0.34673E-04
0.21523E+01 0.70835E+00-0.12219E+01 0.32781E+00 0.36693E-01 0.31919E-02
0.21523E+01 0.37666E-01 0.41418E-01 0.18925E-01 0.17055E-02 0.34673E-04
0.21634E+01 0.70835E+00-0.12219E+01 0.32781E+00 0.36693E-01 0.31919E-02
0.21634E+01 0.37666E-01 0.41418E-01 0.18925E-01 0.17055E-02 0.34673E-04
0.21744E+01 0.70835E+00-0.12219E+01 0.32781E+00 0.36693E-01 0.31919E-02
0.21744E+01 0.37666E-01 0.41418E-01 0.18925E-01 0.17055E-02 0.34673E-04
0.21854E+01 0.70835E+00-0.12219E+01 0.32781E+00 0.36693E-01 0.31919E-02
0.21854E+01 0.37666E-01 0.41418E-01 0.18925E-01 0.17055E-02 0.34673E-04
0.21965E+01 0.70835E+00-0.12219E+01 0.32781E+00 0.36693E-01 0.31919E-02
0.21965E+01 0.37666E-01 0.41418E-01 0.18925E-01 0.17055E-02 0.34673E-04
0.22075E+01 0.70835E+00-0.12219E+01 0.32781E+00 0.36693E-01 0.31919E-02
0.22075E+01 0.37666E-01 0.41418E-01 0.18925E-01 0.17055E-02 0.34673E-04
0.22185E+01 0.70835E+00-0.12219E+01 0.32781E+00 0.36693E-01 0.31919E-02
0.22185E+01 0.37666E-01 0.41418E-01 0.18925E-01 0.17055E-02 0.34673E-04
0.22296E+01 0.70835E+00-0.12219E+01 0.32781E+00 0.36693E-01 0.31919E-02
0.22296E+01 0.37666E-01 0.41418E-01 0.18925E-01 0.17055E-02 0.34673E-04
0.22406E+01 0.70835E+00-0.12219E+01 0.32781E+00 0.36693E-01 0.31919E-02
0.22406E+01 0.37666E-01 0.41418E-01 0.18925E-01 0.17055E-02 0.34673E-04
0.22517E+01 0.70835E+00-0.12219E+01 0.32781E+00 0.36693E-01 0.31919E-02
0.22517E+01 0.37666E-01 0.41418E-01 0.18925E-01 0.17055E-02 0.34673E-04
0.22627E+01 0.70835E+00-0.12219E+01 0.32781E+00 0.36693E-01 0.31919E-02
0.22627E+01 0.37666E-01 0.41418E-01 0.18925E-01 0.17055E-02 0.34673E-04
0.22737E+01 0.70835E+00-0.12219E+01 0.32781E+00 0.36693E-01 0.31919E-02
0.22737E+01 0.37666E-01 0.41418E-01 0.18925E-01 0.17055E-02 0.34673E-04
0.22848E+01 0.70835E+00-0.12219E+01 0.32781E+00 0.36693E-01 0.31919E-02
0.22848E+01 0.37666E-01 0.41418E-01 0.18925E-01 0.17055E-02 0.34673E-04
0.22958E+01 0.70835E+00-0.12219E+01 0.32781E+00 0.36693E-01 0.31919E-02
0.22958E+01 0.37666E-01 0.41418E-01 0.18925E-01 0.17055E-02 0.34673E-04
0.23068E+01 0.70835E+00-0.12219E+01 0.32781E+00 0.36693E-01 0.31919E-02
0.23068E+01 0.37666E-01 0.41418E-01 0.18925E-01 0.17055E-02 0.34673E-04
(z)   Ni at 60 eV
0
20
0.20971E+01-0.12946E+01-0.39032E+00-0.12960E+00 0.27694E+00 0.52215E-01
0.20971E+01 0.36438E-01 0.14401E-01 0.72349E-02 0.57908E-02 0.14905E-02
0.21082E+01-0.12946E+01-0.39032E+00-0.12960E+00 0.27694E+00 0.52215E-01
0.21082E+01 0.36438E-01 0.14401E-01 0.72349E-02 0.57908E-02 0.14905E-02
0.21192E+01-0.12946E+01-0.39032E+00-0.12960E+00 0.27694E+00 0.52215E-01

```

```

0.21192E+01 0.36438E-01 0.14401E-01 0.72349E-02 0.57908E-02 0.14905E-02
0.21302E+01-0.12946E+01-0.39032E+00-0.12960E+00 0.27694E+00 0.52215E-01
0.21302E+01 0.36438E-01 0.14401E-01 0.72349E-02 0.57908E-02 0.14905E-02
0.21413E+01-0.12946E+01-0.39032E+00-0.12960E+00 0.27694E+00 0.52215E-01
0.21413E+01 0.36438E-01 0.14401E-01 0.72349E-02 0.57908E-02 0.14905E-02
0.21523E+01-0.12946E+01-0.39032E+00-0.12960E+00 0.27694E+00 0.52215E-01
0.21523E+01 0.36438E-01 0.14401E-01 0.72349E-02 0.57908E-02 0.14905E-02
0.21634E+01-0.12946E+01-0.39032E+00-0.12960E+00 0.27694E+00 0.52215E-01
0.21634E+01 0.36438E-01 0.14401E-01 0.72349E-02 0.57908E-02 0.14905E-02
0.21744E+01-0.12946E+01-0.39032E+00-0.12960E+00 0.27694E+00 0.52215E-01
0.21744E+01 0.36438E-01 0.14401E-01 0.72349E-02 0.57908E-02 0.14905E-02
0.21854E+01-0.12946E+01-0.39032E+00-0.12960E+00 0.27694E+00 0.52215E-01
0.21854E+01 0.36438E-01 0.14401E-01 0.72349E-02 0.57908E-02 0.14905E-02
0.21965E+01-0.12946E+01-0.39032E+00-0.12960E+00 0.27694E+00 0.52215E-01
0.21965E+01 0.36438E-01 0.14401E-01 0.72349E-02 0.57908E-02 0.14905E-02
0.22075E+01-0.12946E+01-0.39032E+00-0.12960E+00 0.27694E+00 0.52215E-01
0.22075E+01 0.36438E-01 0.14401E-01 0.72349E-02 0.57908E-02 0.14905E-02
0.22185E+01-0.12946E+01-0.39032E+00-0.12960E+00 0.27694E+00 0.52215E-01
0.22185E+01 0.36438E-01 0.14401E-01 0.72349E-02 0.57908E-02 0.14905E-02
0.22296E+01-0.12946E+01-0.39032E+00-0.12960E+00 0.27694E+00 0.52215E-01
0.22296E+01 0.36438E-01 0.14401E-01 0.72349E-02 0.57908E-02 0.14905E-02
0.22406E+01-0.12946E+01-0.39032E+00-0.12960E+00 0.27694E+00 0.52215E-01
0.22406E+01 0.36438E-01 0.14401E-01 0.72349E-02 0.57908E-02 0.14905E-02
0.22517E+01-0.12946E+01-0.39032E+00-0.12960E+00 0.27694E+00 0.52215E-01
0.22517E+01 0.36438E-01 0.14401E-01 0.72349E-02 0.57908E-02 0.14905E-02
0.22627E+01-0.12946E+01-0.39032E+00-0.12960E+00 0.27694E+00 0.52215E-01
0.22627E+01 0.36438E-01 0.14401E-01 0.72349E-02 0.57908E-02 0.14905E-02
0.22737E+01-0.12946E+01-0.39032E+00-0.12960E+00 0.27694E+00 0.52215E-01
0.22737E+01 0.36438E-01 0.14401E-01 0.72349E-02 0.57908E-02 0.14905E-02
0.22848E+01-0.12946E+01-0.39032E+00-0.12960E+00 0.27694E+00 0.52215E-01
0.22848E+01 0.36438E-01 0.14401E-01 0.72349E-02 0.57908E-02 0.14905E-02
0.22958E+01-0.12946E+01-0.39032E+00-0.12960E+00 0.27694E+00 0.52215E-01
0.22958E+01 0.36438E-01 0.14401E-01 0.72349E-02 0.57908E-02 0.14905E-02
0.23068E+01-0.12946E+01-0.39032E+00-0.12960E+00 0.27694E+00 0.52215E-01
0.23068E+01 0.36438E-01 0.14401E-01 0.72349E-02 0.57908E-02 0.14905E-02

```

```

include.out include file: Generated by pad1.f
Used by pad2.f and pad3.f

```

```

C=====
C          Include file: include.out
C          Generated by pad1.f
C          Used by pad2.f and pad3.f
C=====
C
C          PARAMETER(MID=2,MSHL= 6,LMAXP= 4,LOUTP=28,NFRIT=22,LSPDFG=2)
C          PARAMETER(IAXISP=4,MIRP=1,NAMAX=21,NRMAX= 6,NGEO=3)
C          PARAMETER(IPHI=360,IPHIO= 0,ITHETA=90,ITHETA0= 0)
C          PARAMETER(ITSTP= 1,IPSTP= 1)
C          PARAMETER(SRFPNT=2.00,EMFP= 0.0,LCORE= 0)
C
C===== END =====
C

```